RSC Advances

ROYAL SOCIETY OF CHEMISTRY

www.rsc.org/advances

Cite this: DOI: 10.1039/c0xx00000x

www.rsc.org/xxxxxx

ARTICLE TYPE

Pyrene thiazole-conjugate as ratiometric chemosensor with high selectivity and sensitivity for tin (Sn^{4+}) and its application in imaging live cells

Ajit Kumar Mahapatra*,[a] Sanchita Mondal,[a] Kalipada Maiti,[a] Saikat Kumar Manna,[a] Rajkishor Maji,[a] Debasish Mandal,[b] Sukhendu Mandal,[c] Shyamaprosad Goswami,[a] Ching Kheng Quah[d] and Hoong-Kun Fun[d,e]

Received (in XXX, XXX) Xth XXXXXXXXX 20XX, Accepted Xth XXXXXXXXX 20XX
DOI: 10.1039/b000000x

A new pyrene thiazole-conjugate (**PTC**) amine fluoroionophore was synthesized and characterized. The single crystal XRD structure of **PTC** has been established. The fluoroionophore **PTC** showed selectivity toward Sn^{4+} by switch on ratiometric fluorescence among the 15 metal ions studied in HEPES buffer medium with a detection limit of 6.93 μM. The interaction of Sn^{4+} with **PTC** has been further supported by absorption studies, and the stoichiometry of the complex formed (2:1) has been established on the basis of fluorescence and ESI-MS. Competitive ion titrations carried out reveal that the Sn^{4+} can be detected even in the presence of other metal ions of bio-importance. Moreover, the utility of the fluoroionophore **PTC** in showing the tin recognition in live cells has also been demonstrated using Vero 76 cells as monitored by fluorescence imaging. The tin complex of **PTC** was isolated, and the structure and electronic properties of [**PTC**−Sn] has been established by DFT and TDDFT calculations. The isolated tin complex [**PTC**−Sn] has been used as molecular tools for the recognition of anions on the basis of their binding affinities toward Sn^{4+}. [**PTC**−Sn] was found to be sensitive and selective toward sulphide ions among the other 12 anions studied. The selectivity has been shown on the basis of the changes observed in the emission and absorption spectral studies through the removal of Sn^{4+} from [**PTC**−Sn] by S^{2-}.

Introduction

The development of molecular sensors for efficient detection of specific metal ions is an emerging area of particular interest because of their potential analytical applications in many different fields, including chemistry and biology.[1-4] The development of tin (Sn^{4+}) fluorescent chemosensors has attracted intense attention due to the concern over the adverse effect of tin on the environment and human health due to excess accumulation. Tin, widespread in the air, water and soil, is one of the most commonly used heavy metals in agricultural, industry,[5] including food container, food processing equipment, toothpaste, perfumes, soaps, food additives and dyes. Again, organotin compounds are used to make plastics, plastic pipes, PVC stabilizer, pesticides, paints, and pest repellents.[6] Inorganic tin compounds are used as pigments in the ceramic and textile industry.[7] However , human and various animal studies show that excess accumulation of tin can cause eye and skin irritation, headaches, stomachaches and dizziness, breathlessness urination problems, liver damage, malfunctioning of immune systems, chromosomal damage and gastrointestinal effects (abdominal cramps, nausa, diarrhoea, vomiting).[8] Thus, there is a strong need for tin selective chemosensors that rapidly detect Sn^{4+} in aqueous media by simple spectrum analysis. A promising way is to develop optical chemosensors for detecting Sn^{4+} ions, which are based on an indicator that is capable of reporting on the selectivity recognition of Sn^{4+} ions through a variety of optical responses, mainly due to their distinct advantages in sensitivity, selectivity and fluorescence imaging in living cells.

Sulfide anion, as a toxic traditional pollutant, is widely spread in the environment. Sulfide has many applications such as for manufacture of sulfur, sulfuric acid, dyes and cosmetics, but exposure to high level sulfide can lead to a variety of physiological and biochemical problems, including irritation in mucous membranes, unconsciousness, and respiratory paralysis.[9] Once sulfide anion is protonated, it becomes even more toxic. Thus, the detection of sulfide anion has become very important from an industrial, environmental, and biological point of view.[10] Thus, sulfide detection has received enormous interest and a number of detection strategies have been developed for sulfide anions, such as spectroscopy, titration, electrochemical methods, chemoluminescence methods, ion chromatography and etc.[11]

Sulfide sensing by fluorescence spectrometry is an increasingly popular method because of its high sensitivity and easy operability.[12] Although a vast number of S^{2-} selective fluorescent probes have been investigated, fluorescent sensing of sulfide anions in water solution still remains a challenging task due to the strong hydration nature of anions.[13] Fortunately, the displacement (ensemble) approach has been proven to be an effective method to tackle this hurdle. [14]

Therefore, the selective detection of S^{2-} has been a major research focus. Although traditional methods of anion sensing such as the use of ion-selective electrodes has already been discovered, there is an increasing need to find alternative means of analysis, including the use of selective fluorescent chemosensors.[15] In general, sensing anions in aqueous system is much more challenging task than cation due to the strong hydration effects of anions. To date, these studies frequently have adopted the fluorescent complexes containing a transition-metal (such as Sn^{4+}) chelator coupled with a variety of chromophores,[16-17] however, the in situ formed ligand-metal complex has potential utility to act as highly selective anion sensor *via* metal ion displacement approach, which can provide an indirect approach for fluorescence anion detection.

With this in mind and the continuation of our work on the sensing of cations[18] of biological significance, herein we report a novel ratiometric fluorescence chemosensor for S^{2-} using **[PTC**−Sn**]** ensemble based on pyrene thiazole-conjugate units. The selection of thiazole amine in the pyrene platform is based on the considerations that it can function as the potential binding unit for metal ions and pyrene behave as standard fluorophore moiety.[19] For a sensor based on the thiazole moiety, fluorescence is quenched *via* PET from the amine group to the excited singlet state of pyrene. Upon complexation with a suitable metal ion, a large chelation-enhanced-fluorescence (CHEF) effect is observed because chelation abrogates the PET process. So ratiometric fluorescent enhancement (~ 4-fold) was observed upon addition of Sn^{4+} to the solution of **PTC**. **[PTC**−Sn**]** complex also displays selective fluorescent changes for S^{2-} over other tested anions. As a biological application, sensor **PTC** is successfully applied to monitor the intracellular Sn^{4+} ions in cultured Vero 76 cells.

Recently, we presented[18b,d] a displacement-based sensing method by using metal-based receptors for other anion recognition or sensing. The key point is that the stability constant of the complex formed by anion and metal is larger than that of the complex of metal and its chemosensor. From this idea, we have successfully developed a fluoroionophore **PTC** for fluorescence and colorimetric sulphide chemosensors based on the traditional Sn^{4+} chemosensors.

Results and discussion

Compound **2** was readily synthesized in one step by reaction of ketopyrene **1** with $CuBr_2$ in EtOH. The fluoroionophore molecule **PTC** was synthesized in one-step Hantzsch condensation reaction[20] between 1-bromoacetylpyrene with thiourea in ethanol at refluxing condition for 12h. **PTC** has been characterized by various spectral techniques such as ^1H, ^{13}C NMR and high resolution ESI-MS (Experimental section and Fig. S1-S3, ESI†) and its structure has been established by single crystal XRD (Fig. 1).

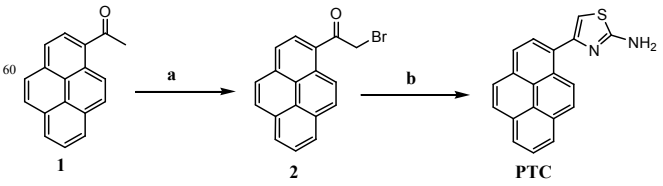

Scheme 1 Scheme for the synthesis of **PTC**: (a) $CuBr_2$, EtOH, heat, 3h; (b) thiourea, dry EtOH, reflux, 12 h.

Single crystals‡ of **PTC** suitable for X-ray diffraction study were obtained by slow eveporation from its MeOH/$CHCl_3$ (1:1) solution. It crystallizes as monoclinic with space group $P2_1/c$. The corresponding details of the structure determination and refinement data are given in Table S1 (S15, ESI†). The XRD structure of **PTC** (Fig. 1) exhibits a twisted conformation with a dihedral angle of 51.31 (6)° between the thiazole ring (S1/N1/C17-C19, r.m.s deviation = 0.006 Å) and the mean plane of the pyrene ring system (C1-C16, r.m.s deviation = 0.041 Å).

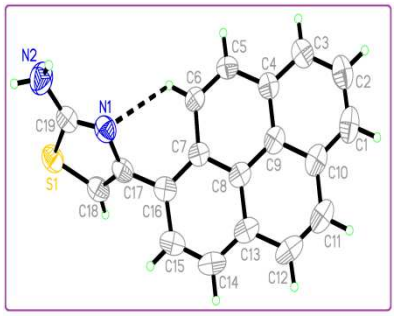

Fig. 1 ORTEP diagram of single crystal XRD structure of **PTC** at 50% ellipsoid probability.

The molecular structure is consolidated by an intramolecular C6—H6*A*···N1 hydrogen bond with distance of 2.10Å, which forms an *S*(6) ring motif.

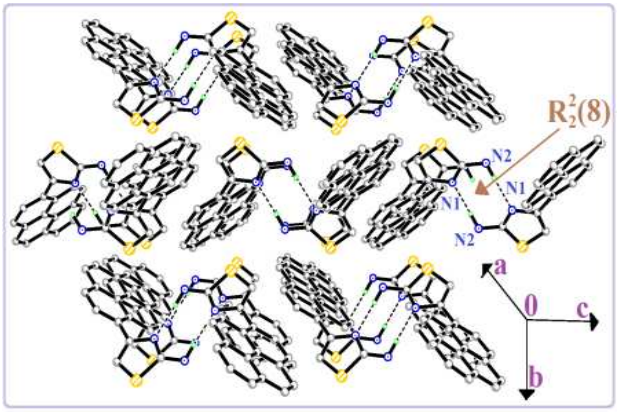

Fig. 2 Crystal packing diagram of **PTC** viewed along [100].

In the crystal packing, the two **PTC** molecules are connected through symmetrical homodimmers by pairs of N2—H2···N1 and N1···H2— N2 by exhibiting hydrogen bond at a distance of 2.49 Å and are stacked along the *a*-axis (Table S2, ESI †) by way of weak aromatic π-π stacking interactions between the benzene rings (C8-C13 & C7/C8/C13-C16) in adjacent molecules with centroid-centroid distances of 3.5741(10) Å. The stacked dimmers possess crystallographic inversion symmetry and generates $R^2_2(8)$ ring motifs (Fig. 2).

The absorption spectra of free **PTC** in EtOH : H_2O solution (4 : 1, v/v, HEPES buffer, pH = 7.4) exhibited different bands from 230 to 350 nm. Absorption titrations were also carried out to support the binding of Sn^{4+} with **PTC**. Addition of Sn^{4+} to a solution of **PTC** in ethanol-water brought changes in its absorption spectra with three absorption bands observed at 242, 277, and 344 nm (Fig. 3A). When **PTC** was titrated against Sn^{4+}, a marginal decrease in the bands at 242, 277, and 344 nm (Fig. 3A).

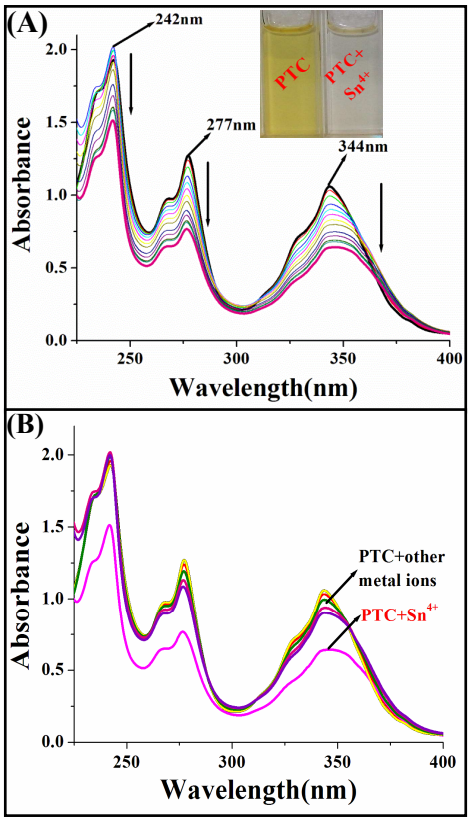

Fig. 3 (A) UV−vis absorption titration spectra of spectra of **PTC** (c = 4 × 10^{-5} M) in aq. EtOH (EtOH/H_2O = 4 : 1, v/v, 10 mM HEPES buffer, pH = 7.4) upon addition of Sn^{4+} (c = 2 × 10^{-4} M). Inset: Photograph of **PTC** and **PTC** + Sn^{4+}. (B) Competitive absorption spectra of **PTC** in the presence of different metal ions (perchlorate, chloride, or nitrate salts of Cr^{3+}, Mg^{2+}, Ca^{2+}, Al^{3+}, Mn^{2+}, Fe^{2+}, Fe^{3+}, Co^{2+}, Ni^{2+}, Cu^{2+}, Zn^{2+}, Cd^{2+}, Hg^{2+}, Ag^{+}, and Pb^{2+}) in aq. EtOH (EtOH/H_2O = 4 : 1, v/v, 10 mM HEPES buffer, pH = 7.4).

However the absorption titration carried out with all the other metal ions showed no significant change, indicating their noninteractive nature with **PTC** (Fig. 3B).The binding affinity of Sn^{4+} toward **PTC** have also been calculated from the Benesi−Hildebrand equation using absorption data and found to have the association constant of 2.22×10^4 M^{-1} (Fig. S10A, ESI†).

Compound **PTC** exhibits a very weak fluorescence in EtOH-water (4 : 1 v/v in HEPES buffer) when excited at λ_{ext} = 344 nm. The emission spectrum shows typical bands at 386 and 402 nm, attributed to the pyrene monomeric emission, and a red-shifted structureless maximum at 485 nm, typical of pyrene dynamic excimer fluorescence,[21] due to the formation of excimers through π−π* interaction between two pyrene molecules[22] with low quantum yield [φ_x(PTC) = 0.0577] (S16, ESI †).

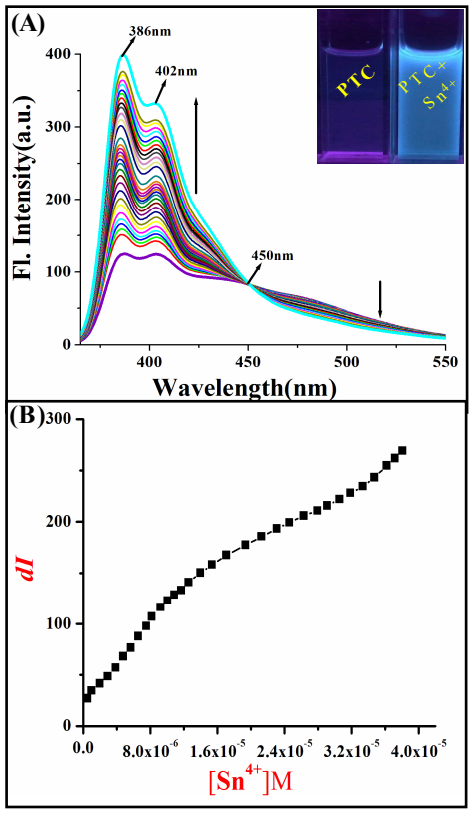

Fig. 4 (A) Fluorescence emission spectra of **PTC** (c = 4 × 10^{-5} M) in aq. EtOH (EtOH/H_2O = 4 : 1, v/v, 10 mM HEPES buffer, pH = 7.4) upon addition of Sn^{4+} (c = 2 × 10^{-4} M). Inset: Fluorescence photographs of **PTC** and **PTC** + Sn^{4+}. (B) change of emission intensity at 386 nm with incremental addition of Sn^{4+} (λ_{ext} = 344 nm).

Titration of **PTC** with Sn^{4+} results in the sizable enhancement of fluorescence intensity at 386 nm as a function of the added Sn^{4+} concentration [($I_{complex}/I_{free\ ligand}$) ~ 4-fold] (Fig. 4A) with a simultaneous decrease of the intensity of pyrene excimer emission at 485 nm. These results imply that the binding of Sn^{4+} at the thiazole part of **PTC** might divide the two pyrene groups

to separate from each other and lack of π-π* stacking between pyrene molecules in this dilute condition, thus causing a decreased excimer emission but an increased monomer emission. Furthermore, it is suggested that during the titration with Sn^{4+}, the metal ion is chelated through thiazole nitrogen and the amine nitrogen, resulting in the utilization of lone pair of the nitrogen to block the PET and thereby the fluorescence enhancement. From the emission titration experiment, the association constant[23] (*Ka*) of **PTC** with Sn^{4+} was estimated to be 4.86×10^4 M^{-1} (Fig. S10B, ESI†). During the titration, the concentration of **PTC** was kept constant at 40 μM and the mole ratio of Sn^{4+} was varied (Fig. 4B). The stoichiometry of the complex system was also determined by the changes in the fluorogenic response of **PTC** in the presence of varying concentrations of Sn^{4+} and the results obtained indicate the formation of a 2 : 1 complex. The Job's plot shows that sensor **PTC** forms a 2 : 1 stoichiometric complexation with Sn^{4+} (Fig. S7, ESI†).[24]

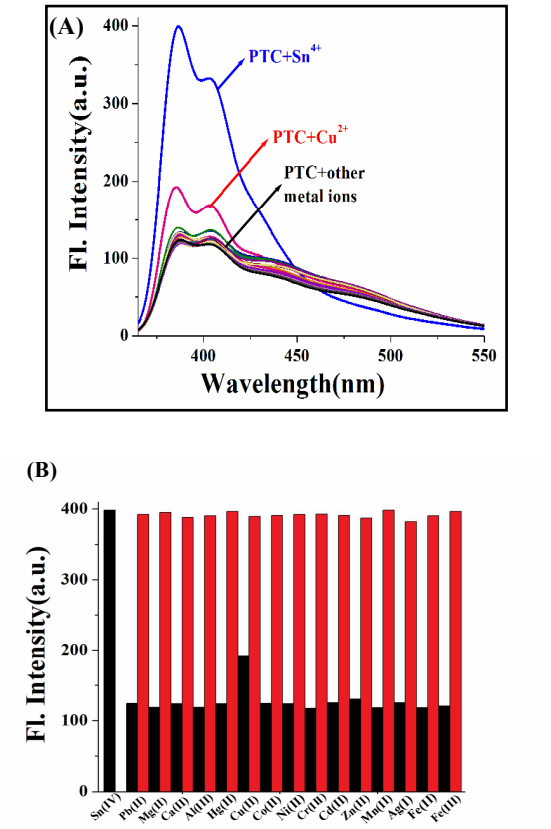

Fig. 5 (A) Competitive fluorescence spectra of **PTC** in the presence of different metal ions (perchlorate, chloride, or nitrate salts of Cr^{3+}, Mg^{2+}, Ca^{2+}, Al^{3+}, Mn^{2+}, Fe^{2+}, Fe^{3+}, Co^{2+}, Ni^{2+}, Cu^{2+}, Zn^{2+}, Cd^{2+}, Hg^{2+}, Ag^{+}, and Pb^{2+}) in aq. EtOH (EtOH/H_2O = 4 : 1, v/v, 10 mM HEPES buffer, pH = 7.4). **5** (B) Histograms showing the fluorescence intensity (I_{386} nm) of **PTC** (c = 4×10^{-5} M) to 4 equiv. addition of Sn^{4+} (c = 2×10^{-4} M) and 10 equiv. of other metal ions (c = 2×10^{-4} M) [the black bar portion] and to the mixture of 10 equiv. of other divalent metal ions with 4 equiv. addition of Sn^{4+} [the red bar portion].

The formation of a 2 : 1 binding mode of the sensor with Sn^{4+} was also confirmed by the ESI-MS mass spectrum (Fig. S5, ESI†), where the spectrum shows a molecular ion peak at m/z of 737.1694 (calc. 737.5022) (Fig. S5, ESI†). The mass spectrum is assignable to the mass of $[2\mathbf{PTC} + Sn^{4+} + NH_4^+]^+$. Therefore, we suggest that probe **PTC** coordinates with Sn^{4+} with 2:1 stoichiometry. The detection limit (LOD) was measured to be 6.93 μM level in the aqueous ethanolic solution (Fig. S11, ESI†). We then proceeded to examine the selectivity of the sensor. The selectivity of compound **PTC** to the various metal ions were tested as selectivity is an important characteristic feature of an ion- selective chemosensor.

We tested our chemosensor with possible interferences including metal ion salts of Ca^{2+}, Mg^{2+}, Cr^{3+}, Al^{3+}, Mn^{2+}, Fe^{2+}, Fe^{3+}, Co^{2+}, Ni^{2+}, Cu^{2+}, Zn^{2+}, Cd^{2+}, Hg^{2+}, Pb^{2+} and Ag^{+} in aq EtOH (EtOH/H_2O = 4 : 1, v/v, 10 mM HEPES buffer, pH = 7.4) (Fig. 5A). Remarkably, only Sn^{4+} elicited a large fluorescence enhancement. By contrast, other metal ions even in the presence of large excess (50 equiv.) have no observable fluorescence response. Furthermore, sensor **PTC** gave only a minimal response to Cu^{2+}, indicating that the sensor is highly selective.

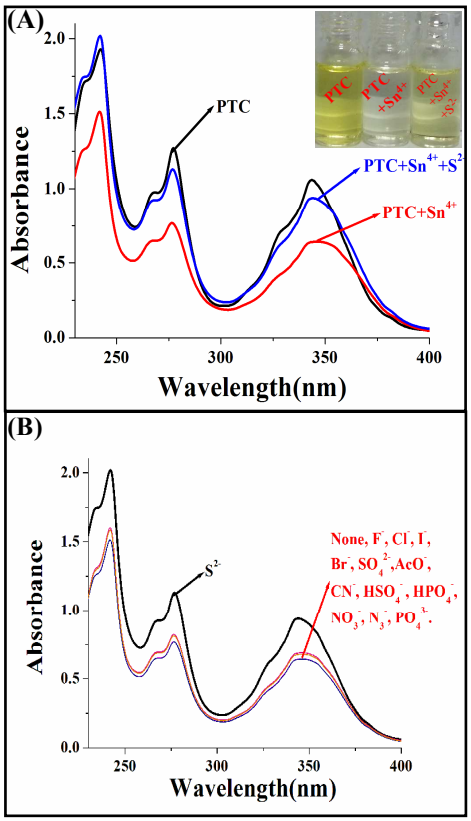

Fig. 6 (A) UV−vis titration spectra of **PTC** (c = 4×10^{-5} M) with 4 equiv. of Sn^{4+} upon addition of sodium sulfide (c = 2×10^{-4} M) in aq. EtOH (EtOH/H_2O = 4 : 1, v/v, 10 mM HEPES buffer, pH = 7.4). Inset: Photographs of **PTC**, **PTC**+ Sn^{4+}, **PTC**+ Sn^{4+}+ S^{2-} in color changes. (B) Changes in the absorption spectra of **PTC**−Sn complex in presence of different anions.

To explore the utility of **PTC** as an ion-selective chemsensor, the

competition experiments was carried out by adding Sn^{4+} to **PTC** solution in presence of other competitive metal ions (Fig. 5B). None of these metal ions significantly affect the emission intensity of **PTC** upon the addition of Sn^{4+}, and the titration profile is similar to that obtained for simple Sn^{4+} titration (Fig. 5B). Therefore, it can be concluded that **PTC** recognizes Sn^{4+} even in the presence of other metal ions.

Interestingly, a solution of **PTC** in optimized EtOH : H_2O solution (4 : 1, v/v, HEPES buffer, pH = 7.4) is pale-yellow and emits light-blue fluorescent light, but during the fluorometric titration of **PTC** with Sn^{4+} ions, the ligth-blue color solution of the receptor became deep sky-blue fluorescent (Fig. 4A inset). This sky-blue fluorescent color is attributed to the excimer of the pyrene moiety.[25]

The chemo-sensing ensemble has been prepared by mixing the 1:2 mole ratio of Sn^{4+} and **PTC** in the EtOH : H_2O solution (4 : 1, v/v, HEPES buffer, pH = 7.4) (Experimental section).

The [**PTC**-Sn] (Fig.4A) was found to be highly fluorescent and thus used for solution studies carried out with anions.

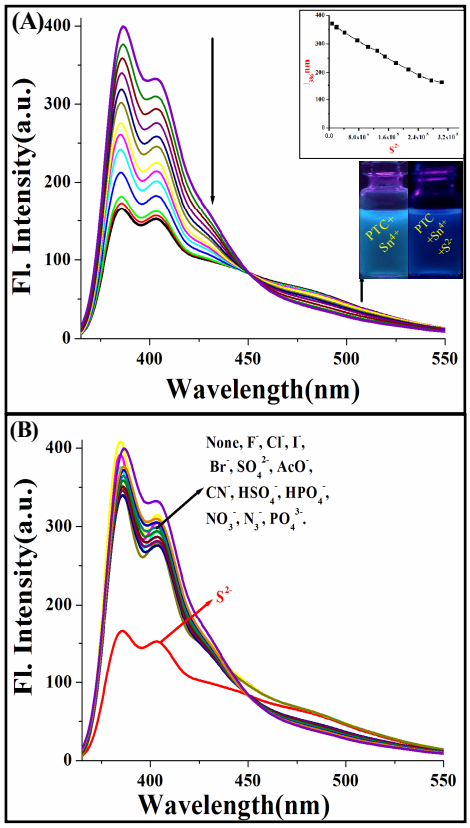

Fig. 7 (A) Fluorescence spectra of **PTC** (c = 4× 10^{-5} M) with 4 equiv. of Sn^{4+} upon addition of sodium sulfide (c =2× 10^{-4} M) in aq. EtOH (EtOH/H_2O = 4:1, v/v, 10 mM HEPES buffer, pH = 7.4). Inset: Change in the fluorescence intensity at 386 nm, 402 nm with incremental addition of Sn^{4+} (λ_{ext} = 344 nm). (B) Changes in the fluorescence spectra of **PTC**−Sn complex in presence of different anions.

Hence, from the above-mentioned studies, we can conclude that **PTC** selectively binds with Sn^{4+} to form **PTC**-Sn complex with considerable change in its spectral properties. We have further studied the influence of different anions on the rupture of this metal−ligand complex and their effect on the reversibility of this complex to regenerate **PTC**. The optical properties of the **PTC**-Sn complex were studied in presence of different anions such as F^-, Cl^-, Br^-, I^-, NO_3^-, N_3^-, S^{2-}, SO_4^{2-}, PO_4^{3-},CH_3COO^- and HPO_4^-, HSO_4^-, CN^-. It is worth mentioning that the regeneration of compound **PTC** is observed only by adding S^{2-} to the solution containing **PTC**-Sn (Fig. 6A), whereas other anions failed to produce any noticeable spectral change (Fig. 6B).

For further understanding, a solution of **PTC** in EtOH : H_2O solution (4 : 1, v/v, HEPES buffer, pH = 7.4) containing > 2 equiv. of Sn^{4+} is titrated in the presence of sulfide anions. The UV−vis spectral pattern of the titration experiment (Fig. 6A) was similar but in reverse direction to the titration curve obtained with Sn^{4+} (Fig. 3A). This fact is evidence that fluoroionophore **PTC** is regained from complex in presence of S^{2-}.

Apart from the results obtained from UV−vis studies, the fluorescence spectroscopy also shows that the emission of the **PTC**-Sn complex returns to its native **PTC** state, selectively in the presence of sulfide anions (Fig. 7A). To further understand the fluorescence "ON−OFF" switching property of the sensor, we have performed fluorescence titration experiment. The fluorescence intensity of the compound **PTC** is enhanced to a moderate level in presence of >1 equiv. of Sn^{4+} ions; the resulting **PTC**−Sn complex is then titrated by the addition of various amounts of sulfide ions. (Fig. 7A), shows that the intensity of the fluorescence emission decreases at 386 nm with increasing concentration of sulfide anion, and on addition of nearly about 4 equiv. of S^{2-} anion, both the intensity and overall pattern of emission spectrum closely match those of compound **PTC** (Fig. 4A), so the fluorescence intensity along with the maximum emission peak are totally regenerated. This showed that Sn^{4+} was released from complex [**PTC**−Sn], and SnS_2 formed. Thus the [**PTC**−Sn] complex acts as a secondary recognition ensemble toward sulphide ions. The results of the spectroscopic studies indicated that the chemosensor **PTC** was recycled during the detection of sulfide anions.

An important property of the chemosensor is highly selectivity towards the analyte as well as the reversibility and reusability in the complexation of any probe to be employed as a chemical sensor for detection of specific metal ions. Therefore, we have further studied the influence of different anions on the rupture of this metal−ligand complex and their effect on the reversibility of [**PTC**−Sn] complex to regenerate **PTC** (Fig. S6, ESI†). It is very exciting and noteworthy that compound **PTC** could be regenerated only by adding Na_2S to the solution containing [**PTC**−Sn].

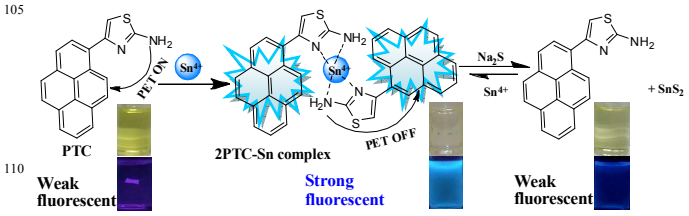

Scheme 2 Schematic presentation showing the possible binding mechanism of **PTC** with Sn^{4+}.

The chemical reversibility behavior of the chemosensor with Sn^{4+}, followed by the removal of Sn^{4+} by S^{2-}, was studied in EtOH : H_2O solution (4 : 1, v/v, HEPES buffer, pH = 7.4).

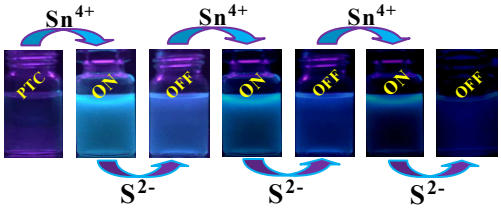

Fig. 8 Fluorescence experiment showing on–off reversible visual fluorescent color changes after each addition of Sn^{4+} and S^{2-} sequentially.

The switch-on and -off action of **PTC** could be studied by monitoring the fluorescence changes as a function of the addition of Sn^{4+} followed by S^{2-}, for four consecutive cycles, wherein remarkable reversal of the fluorescence intensity was observed (Fig. 8).

Hence, **PTC** is a reversible and reusable sensor for Sn^{4+} and its tin complex [**PTC**−Sn] as a secondary sensor for S^{2-}. Like Na_2S, addition of aq. solutions Na_2EDTA brought about almost similar change in emission spectra (Fig. S12, ESI†) and further confirmed the reversibility in the binding process.

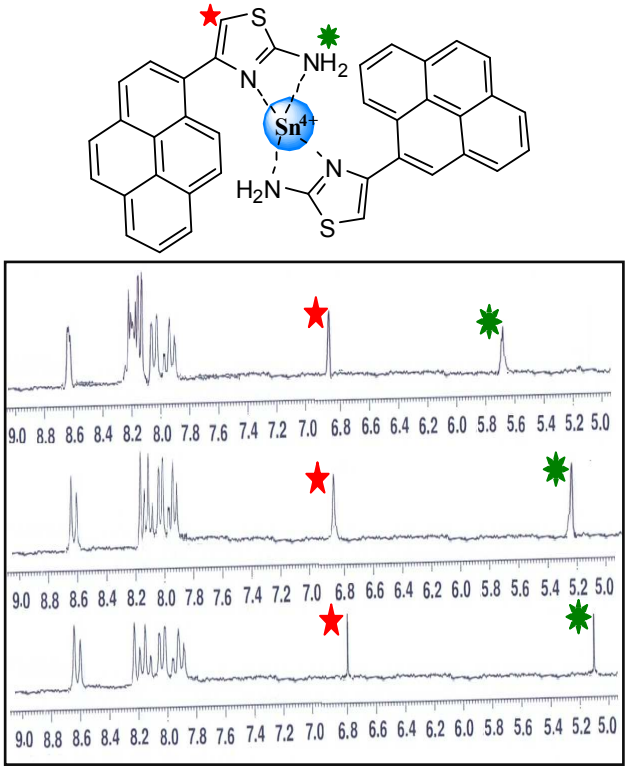

Fig. 9 ^1H NMR spectra measured during the titration of **PTC** with different equivalents of Sn^{4+} (in DMSO-d6): (a) 0; (b) 0.5; (c) 2.0.

The nature of binding of Sn^{4+} to **PTC** has been further studied by ^1H NMR titration by keeping a fixed concentration of **PTC** and varying the amount of Sn^{4+} added to reach up to 2 equiv. During the titration, significant changes were observed in the ^1H NMR spectrum of **PTC** upon addition of Sn^{4+} (Fig. 9). The thiazole –NH_2 proton signals of **PTC** observed at 5.1 ppm are found to shift downfield by about 0.6 ppm, indicating the involvement of the thiazole –NH_2 moiety in Sn^{4+} binding.

Aromatic signals of the thiazole moiety (─CH proton at 6.8 ppm) experiences down field shift in the presence of Sn^{4+} that may arise due to complex formation upon interaction of **PTC** with Sn^{4+}. Again, ^1H NMR titrations were also carried out to check the removal of Sn^{4+} from [**PTC-Sn**] by S^{2-}. For this purpose addition of 2 equiv of sulfide anions to the ensemble solution, the resulted product of [**PTC+ Sn+ S^{2-}**] was isolated by a silica gel column and was then subjected to ^1H NMR analysis (Fig. S4, ESI†). The ^1H NMR of the resulting product is essentially identical to that of free **PTC** and thus clearly supporting Sn^{4+} removal from its complex by releasing free **PTC**.

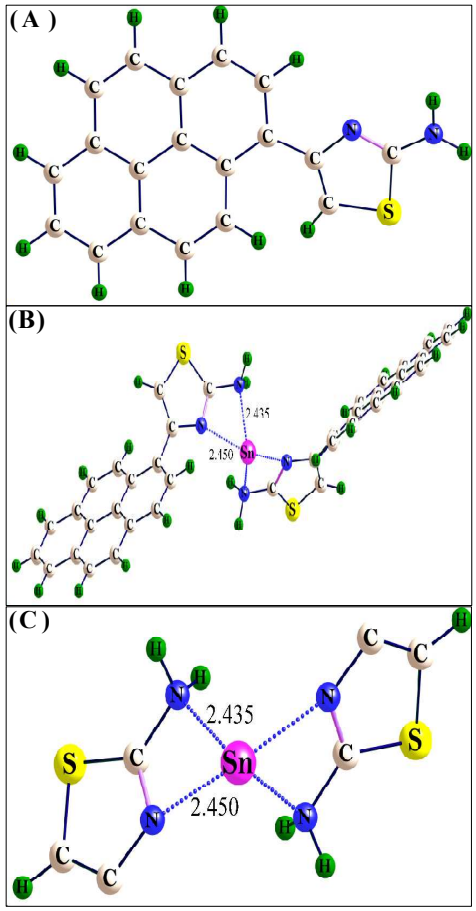

Fig. 10 Calculated energy-minimized structure of (A) **PTC**; (B) [**PTC**-Sn] complex; and (C) the binding core around Sn^{4+}.

As the stiochiometry of the complex formed between Sn^{4+} and **PTC** was found to be 1 : 2 based on emission, absorption, and ESI-MS studies, the structural features of the complex formed between **PTC** and the Sn^{4+} were addressed computational calculations with the B3LYP[26] hybrid density functional employing 6-31G* basis for all atom excluding Sn. For Sn Lanl2dz basis set and pseudo potential are used for Sn. All the calculations have been performed using a suite of Gaussian 09

software package.[27] The geometry optimizations for **PTC** and [**PTC**−Sn] complex were done in a cascade fashion starting from semiempirical PM2 followed by *ab initio* HF to DFT B3LYP by using various basis sets, *viz*., PM2 →HF/STO-3G → HF/3-21G → HF/ 6-31G → B3LYP/ 6-31G(*d,p*). Initially the crystal structure of **PTC** was optimized by DFT.

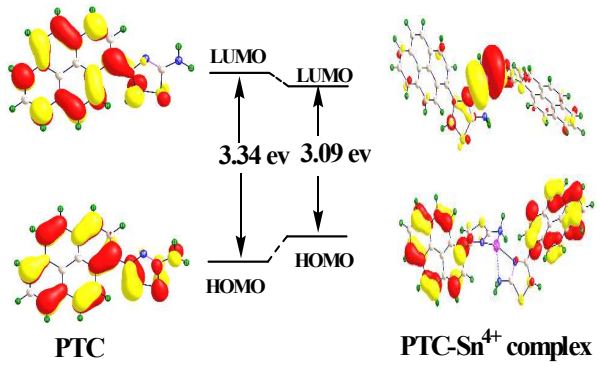

Fig. 11 HOMO and LUMO distributions of **PTC** and **PTC**−Sn^{4+} complex.

The optimized **PTC** was subjected to the interaction with Sn^{4+}, and the corresponding complex was further optimized. In the optimized structure of [**PTC**−Sn], the Sn^{4+} was found in an N_4 core with a distorted tetrahedral geometry around Sn^{4+} where all four bonds (2×Sn-$N_{thiazole}$ and 2×Sn-N_{NH2}) are bonded to the central ion with their distances of 2.45 and 2.43 Å respectively (Fig. 10c). The π electrons distribution and orbital energies of HOMO and LUMO of **PTC** and [**PTC**−Sn] were also determined (Fig 11). The π electrons on the HOMO of **PTC**−Sn complex is mainly located on the whole π-conjugated pyrene framework, but the LUMO is mostly positioned at the center of the guest Sn^{4+} ion. Moreover, the HOMO−LUMO energy gap of complex becomes much smaller relative to that of probe **PTC**. The energy gaps between HOMO and LUMO in the probe **PTC** and [**PTC**−Sn] complex were 3.34 eV and 3.09 eV respectively (S14, ESI†). The result clearly suggest that the Sn^{4+} ion binds to **PTC** very well through four coordination sites, and the whole molecular system forms a nearly planar structure. Hence, the interaction of the thiazole N atom with Sn^{4+} can change the orbital energy level, realizing the optical detection. In addition, time dependent DFT (TDDFT) calculations indicate that **PTC** has a strong absorption band at long wavelength [*f* (oscillator strength) = 0.412] attributed to the S1←S0 transition and two weak absorption bands at short wavelength (*f* = 0.306 and *f* = 0.484) are assigned to the S15←S0 and S18←S0 transitions respectively. Thus, the results of TDDFT calculations are in good agreement with the absorption spectra of **PTC** observed experimentally (S14, ESI†).

The fluorescence images were recorded before and after the addition of Sn^{4+} (20 μM) (Fig. 12). Vero 76 cells incubated with chemosensor **PTC** exhibited no fluorescence, whereas a bright fluorescence signal was observed in the cells stained with chemosensor **PTC** and Sn^{4+}, which in good agreement with the fluorescence turn-on profile of the sensor in the presence of Sn^{4+} in the solution.

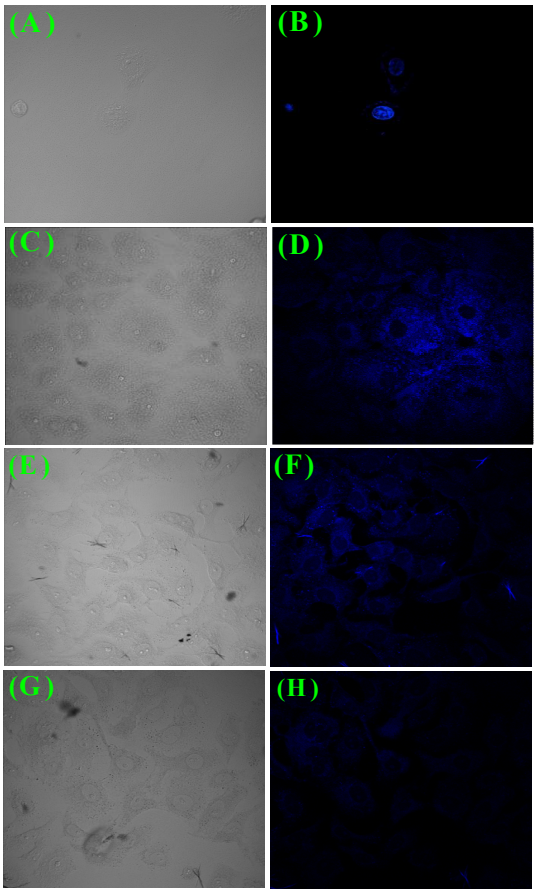

Fig. 12. Confocal microscopic images of probe Pyrene-amine in Vero 76 cells pretreated with Sn: (A) bright field image of the cells of controlled set treated with Sn at 1×10^{-4} M concentration, (B) treated with Sn at 1×10^{-4} M concentration, nuclei counterstained with DAPI (1 μg/mL), (C) bright field image of Sn pretreated cell further treated with Pyrene-amine at 1.0×10^{-6} M concentration, (D) cells of C scanned with Ex = 405 nm and Em = 461 nm, (E) bright field image of the cells treated with probe Pyrene-amine at concentration 1.0×10^{-6} M and further treatment with Na_2S at concentration 1.0×10^{-5} M, (F) cells of E scanned with Ex = 405 nm and Em = 461 nm, (G) bright field image of the cells stained with probe pyrene-amine at concentration 1.0×10^{-6} M and treatment with Na_2S at concentration 1.0×10^{-5} M, (H) cells of G detected at Ex = 405 , Em = 461. All images were acquired with a 60x objective lens.

Moreover, blue-colored fluorescence cells obtained from the incubation of the receptor **PTC** followed by treatment with Sn^{4+} became invisible in fluorescence upon addition of Na_2S (30 μM) (Fig. 12). The results establish that chemosensor **PTC** is cell membrane permeable and can be efficiently used for in vitro imaging of tin ions in living cells. Moreover, there were no indications of cell damage. Cells were intact and showed healthy spread and adherent morphology during and after the labeling process with chemosensor **PTC**, indicating an absence of cytotoxic effects (Fig. S13, ESI†).

Conclusion

A structurally characterized pyrene thiazole−cojugate of **PTC** exhibits high selectivity toward Sn^{4+}. The selectivity has been demonstrated by fluorescence, absorption, ^1H NMR and ESI-MS spectroscopy. Interaction of Sn^{4+} with **PTC** enhances the fluorescence emission at 386 nm, 402 nm and induces a turn on response in electronic and fluorescence spectra in the visible region. At the same time a new structureless emission band at 485 nm was gradually decreased due to the disappearance of the pyrene excimer emission on dilution. **PTC** is sensitive and selective toward Sn^{4+} over other biologically important ions studied, *viz*., Ca^{2+}, Mg^{2+}, Cr^{3+}, Al^{3+}, Mn^{2+}, Fe^{2+}, Fe^{3+}, Co^{2+}, Ni^{2+}, Cu^{2+}, Zn^{2+}, Cd^{2+}, Hg^{2+}, Pb^{2+} and Ag^{+} ions, as demonstrated by individual as well as competitive metal ion titrations. Thus, these receptors could be used as a dual probe for visual detection through change in color and fluorescence. Whereas the fluorescence and absorption spectroscopy provided information for the formation of 1 : 2 complex between Sn^{4+} and **PTC**, *viz*., [**PTC**−Sn], the ESI-MS confirmed the formation unambiguously by exhibiting the correct peak pattern for the presence of tin in the complex. The fluorescent tin complex of **PTC**, *viz*., [**PTC**−Sn], have been subjected to studies of their secondary sensing properties toward various anions. This ensemble was able to detect S^{2-} in exactly the reverse manner to what happens when Sn^{4+} is added to **PTC** in fluorescence spectroscopy. The selectivity has been shown on the basis of fluorescence, absorption, visual color change, ^1H NMR, and cell intake studies. Hence, the effectiveness of compound **PTC** as a probe for intracellular detection of Sn^{4+} by fluorescence microscopy was also studied and presented.

Experimental Section

General Information and Materials

The ^1H and ^{13}C NMR spectra were measured on Bruker–400 MHz spectrometer. Mass spectra were carried out using a Water's QTOF Micro YA 263 mass spectrometer. UV–visible and fluorescence spectra measurements were performed on a SHIMADZU UV-1800 and a Perkin Elmer LS55 spectrofluorimeter respectively. Single crystal X-raydiffraction data for **PTC** were collected on Bruker APEX II Duo CCD area-detector diffractometer at 294K temperature.

All cationic compound such as perchlorate of Mg^{2+}, Cu^{2+}, Fe^{2+}, Co^{2+}, Ni^{2+}, Mn^{2+}, Hg^{2+}, Zn^{2+}, chlorides of Ca^{2+}, Cr^{3+}, Cd^{2+}, Fe^{3+}, Pb^{2+}, Sn^{4+}, nitrate salts of Ag^{+}, Al^{3+}, sodium salts of S^{2-} and di-sodiumsalts of EDTA were purchased from a commercial supplier, stored in a desiccators under vacuum containing self-indicating silica, and used without any further purification. For spectrophotometer measurements, EtOH (Spectrochem) and Elix Millipore water were used as solvents throughout all experiments. . The ^1H NMR spectra were recorded on Bruker 400 MHz spectrometer. Mass spectra were carried out using a Waters QTOF Micro YA 263 mass spectrometer. The ^1H NMR chemical shift values are expressed in ppm (δ) relative to $CHCl_3$ (δ = 7.26 ppm). The following abbreviations are used to describe spin multiplicities in ^1H NMR spectra: s = singlet; d = doublet; t = triplet; m = multiplet.

Preparation of Test solution for UV-vis and fluorescence study. A stock solution of the probe **PTC** (4.0×10^{-5} M) was prepared in EtOH/H_2O (4:1, v/v). All experiments were carried out in EtOH–H_2O solution (EtOH : H_2O = 4 : 1, v/v, 10mM HEPES buffer, pH = 7.4). In titration experiments, each time a 4 $\times 10^{-5}$ M solution of **PTC** was filled in a quartz optical cell of 1 cm optical path length, and the ion stock solutions were added into the quartz optical cell gradually by using a micropipette. Spectral data were recorded at 1 min after the addition of the ions. In selectivity experiments, the test samples were prepared by placing appropriate amounts of the anions/cations (2×10^{-4} M) stock into 2 mL of solution of **PTC** (4×10^{-5} M).

Computational Studies. All geometries for **PTC** and **PTC**-Sn^{4+} were optimized by density functional theory (DFT) calculations using Gaussian 09 (B3LYP/6-31G(*d,p*)) software package.[27]

Cell Culture. Vero cell (very thin endothelial cell) (Vero 76, ATCC No CRL-1587) lines were prepared from continuous culture in Dulbecco's modified Eagle's medium (DMEM, Sigma Chemical Co., St. Louis, MO) supplemented with 10% fetal bovine serum (Invitrogen), penicillin (100 µg/mL), and streptomycin (100 µg/mL). The Vero 76 were obtained from the American Type Culture Collection (Rockville, MD) and maintained in DMEM containing 10% (v/v) fetal bovine serum and antibiotics in a CO_2 incubator. Cells were initially propagated in 75 cm^2 polystyrene, filter-capped tissue culture flask in an atmosphere of 5% CO_2 and 95% air at 37°C in CO_2 incubator. When the cells reached the logarithmic phase, the cell density was adjusted to 1.0x 10^5 per/well in culture media. The cells were then used to inoculate in a glass bottom dish, with 1.0 mL (1.0×10^4 cells) of cell suspension in each dish. After cell adhesion, culture medium was removed. The cell layer was rinsed twice with phosphate buffered saline (PBS), and then treated according to the experimental need.

Cell Imaging Study. For confocal imaging studies Vero cells, 1 x10^4 cells in 1000 µL of medium, were seeded on sterile 35 mm covered Petridis, glass bottom culture dish (ibidi GmbH, Germany), and incubated at 37°C in a CO_2 incubator for 10 hours. Then cells were washed with 500 µL DMEM followed by incubation with 1.0 x10^{-4} M $SnCl_4$ dissolved in 500 µL DMEM at 37°C for 1 h in a CO_2 incubator and observed under an Olympus IX81 microscope equipped with a FV1000 confocal system using 1003 oil immersion Plan Apo (N.A. 1.45) objectives. Images obtained through section scanning were analyzed by Olympus Fluoview (version 3.1a; Tokyo, Japan) with excitation at 405 nm monochromatic laser beam. The cells were again washed thrice with phosphate buffered saline PBS (pH 7.4) to remove any free $SnCl_4$ and incubated in PBS containing probe **PTC** to a final concentrations of 1.0 x 10^{-6} M, incubated for 10 min followed by washing with PBS three times to remove excess probe outside the cells and images were captured. In a separate culture dish undergoing the same treatment the cells were then treated with

1.0×10^{-5} M of Na_2S solution for 1 h; the cells were washed with PBS three times to remove free compound and ions before analysis. In separate culture dish the cells were similarly treated with 1.0×10^{-6} M probe **PTC**, incubated for 10 min, washed thrice with PBS and the image was captured to get any possible background fluorescence. According to the need of the experiment we follow similar procedures to label the cell nuclei by treatment with DAPI (1 μg/mL) followed by three times wash with PBS and subsequently image was captured with excitation wavelength of laser was 405 nm, and emission was 461 nm. For all images, the confocal microscope settings, such as transmission density, and scan speed, were held constant to compare the relative intensity of intracellular fluorescence.

Cytotoxicity Assay. The cytotoxic effects of probe **PTC**, $SnCl_4$, and **PTC**-Sn^{4+}complex were determined by an MTT [3-(4,5-dimethylthiazol-2-yl)-2,5-diphenyltetrazolium bromide] assay following the manufacturer's instruction (MTT 2003, Sigma-Aldrich, MO). Vero cells were cultured into 96-well plates (10^4 cells per well) for 24 h. After overnight incubation, the medium was removed, and various concentrations of **PTC**, $SnCl_4$, and **PTC**-Sn^{4+} complex (0, 5, 25, 50, 75, and 100 μM) made in DMEM were added to the cells and incubated for 24 h. Control experiments were set with DMSO, cells without any treatment and cell-free medium were also included in the study. Following incubation, the growth medium was removed, and fresh DMEM containing MTT solution was added. The plate was incubated for 3−4 h at 37°C. Subsequently, the supernatant was removed, the insoluble colored formazan product was solubilized in DMSO, and its absorbance was measured in a microplate reader (Perkin-Elmer) at 570 nm. The assay was performed in triplicate for each concentration of **PTC**, $SnCl_4$, and **PTC**-Sn^{4+}. The OD value of wells containing only DMEM medium was subtracted from all readings to get rid of the background influence. The cell viability was calculated by the following formula: (mean OD in treated wells / mean OD in control wells) X 100.

Synthesis of chemosensor PTC. Compound 2(1-bromoacetylpyrene) was synthesized according to literature methods.[20] A mixture of compound 2 (1-bromoacetylpyrene) (0.200 g, 0.619 mmol) and Thiourea (0.056 g, 0.7428 mmol) in 15 ml absolute ethanol was refluxed for 12 h. After the completion of the reaction (monitored by TLC), solvent was evaporated and the reaction mixture was poured into ice-water, and powdered product were extracted with $CHCl_3$. The organic layer was washed with saturated NaCl aq. Solution, dried over anhydrous $MgSO_4$ and evaporated to give a yellow solid which was crystallized from MeOH/$CHCl_3$ (1 : 1) solution to give compound **PTC** in 65% yield; M.P. > 250°C. ^{1}H NMR (400 MHz, $CDCl_3$, $Si(CH_3)_4$, J (Hz), δ(ppm)): 8.65 (1H, d, J=9.32Hz), 8.17(4H, m), 8.08 (3H, d, J=10.48 Hz), 8.00 (1H, t, J=7.56 Hz), 6.79 (1H, s,), 5.11 (2H, s, -NH_2). ^{13}C NMR (d_6-DMSO, 500 MHz) δ(ppm): 78.86,105.96, 123.80, 124.08, 124.63, 124.94, 125.11, 125.41, 126.31, 127.17, 127.28, 127.55, 127.68, 128.05, 130.27, 130.69, 130.82, 150.06, 168.79. TOF MS ES$^+$, m/z = 301.0522, [M+H] $^+$, calc. for $C_{19}H_{12}N_2S$ =300.3770.

Acknowledgment

We thank the DST-West Bengal [Project no. 124(Sanc.)/ST/P/S&T/9G-17/2012] for financial support. SKM and SM thanks to the UGC, New Delhi for a fellowship. The authors (HKF) extend their appreciation to the Deanship of Scientific Research at King Saud University for funding this work through research group No. RGP-VPP-207.

Notes and references

[a]Department of Chemistry, Indian Institute of Engineering Science and Technology, Shibpur, Howrah-711103, West Bengal, India, Email: akmahapatra@rediffmail.com, Fax: +913326684564

[b] Institute of Chemistry, The Hebrew University of Jerusalem, 91904 Jerusalem, Israel.

[c] Department of Microbiology, University of Calcutta, Kolkata- 700019.

[d] X-ray Crystallography Unit, School of Physics, Universiti Sains Malaysia, 11800 USM, Penang, Malaysia.

[e] Department of Pharmaceutical Chemistry College of Pharmacy, King Saud University, P.O. Box. 2457, Riyadh 11451 Kingdom of Saudi Arabia.

† Electronic Supplementary Information (ESI) available: [details of any supplementary information available should be included here]. See DOI: 10.1039/b000000x/.

‡Crystal data for **PTC**: CCDC number-1011198. Emperical formula- $C_{19}H_{12}N_2S$. Molecular weight- 300.37. Crystal system, space group- Monoclinic, $P2_1/c$ .Temperature (K)-294. a, b, c (Å)-10.2235 (9), 12.4997 (11), 11.191 (1). β (°)- 100.6620(15). V (Å^3)- 1405.4 (2). Z– 4. Crystal size (mm) - 0.315×0.380×0.603. No. of measured, independent and observed [$I > 2\sigma(I)$] reflections-2346, 2346. R_1, wR_2 (%)- 0.040, 0.124. GOF (F^2)- 1.04. *hkl* range- $h = -12 \rightarrow 12$, $k = -15 \rightarrow 15$, $l = -13 \rightarrow 13$. μ (mm^{-1})- 0.23

1 (a) B. Valeur and I. Leray, *Coord. Chem. Rev.*, 2000, **205**, 3-40. (*b*) E. M. Nolan and S. J. Lippard, *Chem. Rev.,* 2008, **108**, 3443-3480. (c) E. L. Que, D. W. Domaille and C. J. Chang, *Chem. Rev.*, 2008, **108**, 1517-1549. (d) M. Suresh, A. Ghosh, and A. Das, *Chem. Commun.,* 2008, 3906–3908. (e) S. Yoon, A. E. Albers, A. P. Wong, and C. J. Chang, *J. Am. Chem. Soc*., 2005, **127**, 16030–16031.

2 (a) S. Yoon, E. W. Miller, Q. He, P. K. Do and C. J. Chang, *Angew. Chem., Int. Ed*., 2007, **46**, 6658–6651. (b) G. Zhang, D. Zhang, S. Yin, X. Yang, Z. Shuai, and D. Zhu, *Chem. Commun*., 2005, 2161–2163. (c) E. M. Nolan, and S. J. Lippard, *J. Am. Chem. Soc*., 2003, **125**, 14270–14271. (d) A. Descalzo, R. Martinez-Manez, R. Radeglia, K. Rurack, and J. Soto, *J. Am. Chem. Soc*., 2003, **125**, 3418–3419. (e) G. Hennrich, W. Walther, U. Resch-Genger, and H. Sonnenschein, *Inorg. Chem*., 2001, **40**, 641–644.

3 (a) G. Hennrich, H. Sonnenschein, and U. Resch-Genger, *J. Am. Chem. Soc*., 1999, **121**, 5073–5074. (b) V. Dujols, F. Ford, and A. W. Czarnik, *J. Am. Chem. Soc*., 1997, **119**, 7386–7387. (c) J. Y. Kwon, Y. J. Jang, Y. J. Lee, K. M. Kim, M. S. Seo, W. Nam, and J. Yoon, *J. Am. Chem. Soc*., 2005, **127**, 10107–10111. (d) M. Suresh, S. K. Mishra, S. Mishra, and A. Das, *Chem. Commun*., 2009, 2496–2498. (e) A. W. Czarnik, American Chemical Society, Washington, D. C., 1992.

4 (a) A. P. de Silva, D. B. Fox, A. J. M. Huxley, and T. S. Moody, *Coord. Chem. Rev.*, 2000, **205**, 41-57. (b) X. He, H. Liu, Y. Li, S. Wang, Y. Li, N. Wang, J. Xiao, X. Xu, and D. Zhu, *Adv. Mater.*,2005, **17**, 2811-2815. (c) J. R. Miller, J. Rowland, P. J. Lechler, M. Desilers, and L. C. Hsu,

Water,Air, Soil Pollut., 1996, **86**, 373-388. (d) P. B. Tchounwou, W. K. Ayensu, N. Ninashvili, and D. Sutton, *Environ. Toxicol. Chem.*, 2003, **18**, 149-175. (e) A. J. Weerasinghe, C. Schmiesing, and E. Sinn, *Tetrahedron Letters*, 2009, **50**, 6407–6410. (f) R. Kagit, M. Yildirim, O. Ozay, S. Yesilot, and H. Ozay, *Inorg. Chem*., 2014, **53**, 2144–2151. (g) F. Hou, L. Huang, P. Xi, J. Cheng, X. Zhao, G. Xie, Y. Shi, F. Cheng, X. Yao, D. Bai, and Z. Zeng, *Inorg. Chem*., 2012, **51**, 2454−2460.

5 (a) A.-M. Florea, and D. Bu¨sselber, *BioMetals*., 2006, **19**, 419–427. (b) Concise International Chemical Assessment Document 65 by WHO, Geneva, 2006.

6 (a) Y. Arakawa, Sangyo Eiseigaku Zasshi, 1997, **39**, 1-20. (b) ILO. Tin. In: Stellman J, ed. *Encyclopedia of Occupational Health and Safety.* 4th ed. Geneva: International Labour Organization (ILO), 1998, 63:41 pp.

7 JECFA (1989) *Toxicological evaluation of certain food additives and contaminants.* Joint FAO/WHO Expert Committee on Food Additives. Cambridge, Cambridge University Press, pp. 329–336 (WHO Food Additives Series No. 24).

8 (a) Agency for Toxic substances and Disease Registry (ATSDR) 2005. (b) L. R. Herman, J. Masters, R. Peterson, and S. Levine, *J Anal. Toxicol*., 1986, **10**, 6-9. (c) X. Lou, D. Ou, Q. Li, and Z. Li, *Chem. Commun*., 2012, **48**, 8462-8477.

9 (a) Hydrogen Sulfide; World Health Organization: Geneva, 1981 (Environmental Health Criteria, No. 19). (b) X. Cao, W. Lin, and L. He, *Org. Lett*., 2011, **13**, 4716-4719.

10 R. F. Huang, X. W. Zheng and Y. J. Qu, *Anal. Chim. Acta*, 2007, **582**, 267.

11 (a) D. Jiménez, R. Martínez-Máñez, F. Sancenón, J. V. Ros-Lis, A. Benito, and J. Soto, *J. Am. Chem. Soc*., 2003, **125**, 9000-9001. (b) X. Lou, H. Mu, R. Gong, E. Fu, J. Qin, and Z. Li, *Analyst* 2011, **136**, 684-687. (c) L. Zhang, X. Lou, Y. Yu, J. Qin, and Z. Li, *Macromolecules* 2011, **44**, 5186-5193. (d) J. Liu, J. Chen, Z, Fang, and L. Zeng, *Analyst*, 2012, **137**, 5502-5505. (e) J. Zhang, X. Xu, and X. Yang, *Analyst*, 2012, **137**, 1556-1558.

12 (a) G. Zhou, H. Wang, Y. Ma, and X. Chen, *Tetrahedron*, 2013, **69**, 867-870. (b) M.-Q. Wang, K. Li, J.-T. Hou, M.-Y. Wu, Z. Huang, and X.-Q. Yu, *J. Org. Chem*., 2012, **77**, 8350-8354.

13 P. D. Beer, and P. A. Gale, *Angew. Chem. Int. Ed*., 2001, **40**, 486-516.

14 (a) S. L. Wiskur, H. Ait-Haddou, J. J. Lavigne, and E. V. Anslyn, *Acc. Chem. Res*., 2001, **34**, 963-972. (b) A. T. Wright and E. V. Anslyn, *Chem. Soc. Rev*., 2006, **35**, 14-28. (c) X. Lou, D. Ou, Q. Li, and Z. Li, *Chem. Commun*., 2012, **48**, 8462-8477.

15 (a) W. N. Lipscomb and N. Sträter, *Chem. Rev*., 1996, **96**, 2375. (b) P. A. Gale, *Acc. Chem. Res*., 2006, **39**, 465. (c) E. J. O'Neil and B. D. Smith, *Coord. Chem. Rev*., 2006, **250**, 3068. (d) J. Yoon, S. K. Kim, N. J. Singh and K. S. Kim, *Chem. Soc. Rev*., 2006, **35**, 355.

16 Q. Wang, C. Li, Y. Zou, H. Wang, T. Yi, and C. Huang, *Org. Biomol. Chem*., 2012, **10**, 6740-6746.

17 A. K. Mahapatra, S. K. Manna, D. Mandal, and C. D. Mukhopadhyay, *Inorg. Chem*., 2013, **52**, 10825–10834.

18 (a) A. K. Mahapatra, S. K. Manna, S. K. Mukhopadhyay, and A. Banik, *Sens. Actuators B*, 2013, **183**, 350-355. (b) A. K. Mahapatra, J. Roy, P. Sahoo, S. K. Mukhopadhyay and A. Chattopadhyay *Org. Biomol. Chem*., 2012, **10**, 2231. (c) A.K. Mahapatra, S. K. Manna, C. D. Mukhopadhyay, and D. Mandal *Sensors and Actuators B*, 2014, **200**, 123–131. (d) A.K. Mahapatra, S. K. Manna, K. P. Maity, R. K. Maji, C. D. Mukhopadhyay, D. Sarkar, and T. K. Mondal, *RSC Adv*., 2014, **4**, 36615–36622.

19 (a) D. Sahoo, V. Narayanaswami, C. M. Kay, and R. O. Ryan, *Biochemistry*, 2000, **29**, 6594-6601. (b) J. F. Callan, A. P. de Silva, and D. C. Magri, *Tetrahedron*, 2005, **61**, 8551-8588. (c) S.-K. Kim, J.-H. Bok, R. A. Bartsch, J.-Y. Lee and J.-S. Kim, *Org. Lett*., 2005, **7**, 4839. (d) R. Martı´nez, F. Zapata, A. Caballero, A. Espinosa, A. Ta´rraga, and P. Molina, *Org. Lett*., 2006**, 8**, 3235-38.

20 A. Hantzsch, and J. Liebigs, *Ann.Chem.* 1889, **250**, 257-273. (b) G. Schwarz, *Org. Synth. Coll.* 1945, **25**, 35.

21 (a) S. Nishizawa, Y. Kato, and N. Teramae, *J. Am. Chem. Soc*., 1999, **121**, 9463-9464. (b) D. Sahoo, V. Narayanaswami, C. M. Kay, and R. O. Ryan, *Biochemistry*, 2000, 29, 6594-6601. (c) J. F. Callan, A. P. de Silva, and D. C. Magri, *Tetrahedron*, 2005, **61**, 8551-8588.

22 F. M. Winnik, *Chem. Rev*., 1993, **93**, 587−614.

23 (a) B. Valeur, J. Pouget, and J. Bouson, *J. Phys. Chem*., 1992, **96**, 6545-6549. (b) K. A. Connors, and J. Wiley & Sons, Binding Constants─The Measurement of Molecular Complex Stability, New York, 1987. (c) V. K. Indirapriyadharshini, P. Karunanithi, and P. Ramamurthy, *Langmuir*, 2001, **17**, 4056–4060.

24 (a) B. N. Ahamed, M. Arunachalam, and P. Ghosh, *Inorg. Chem*., 2010, **49**, 4447–4457. (b) D. Maity and T. Govindaraju, *Inorg. Chem*., 2011, **50**, 11282–11284

25 (a) A. B. Othman, J. W. Lee, J.-S. Wu, J. S. Kim, R. Abidi, P. Thuéry, J. M. Strub, A. V. Dorsselaer, and J. Vicens, *J. Org. Chem.*, 2007, **72**, 7634. (b) Y. H. Lee, M. H. Lee, J. F. Zhang, and J. S. Kim, *J. Org. Chem*., 2010, **75**, 7159–7165. (c) S. H. Lee, S. H. Kim, S. K. Kim, J. H. Jung, and J. S. Kim, *J.Org.Chem*., 2005, **70**, 9288-9295.

26 (a) A. D. Becke, *J. Chem. Phys*., 1993, **98**, 5648. (b) C. Lee, W. Yang and R. G. Parr, *Phys. Rev. B*, 1988, **37**, 785. (c) D. Andrae, U. 35 Haeussermann, M. Dolg, H. Stoll and H. Preuss, *Theor.Chim.Acta*,1990, **77**, 123.

27 M. J. Frisch, G. W. Trucks, H. B. Schlegel, G. E. Scuseria, M. A. Robb, J. R. Cheeseman, G. Scalmani, V. Barone, B. Mennucci, G. A. Petersson, H. Nakatsuji, M. Caricato, X. Li, H. P. Hratchian, A. F. Izmaylov, J. Bloino, G. Zheng, J. L. Sonnenberg, M. Hada, M. Ehara, K. Toyota, R. Fukuda, J. Hasegawa, M. Ishida, T. Nakajima, Y. Honda, O. Kitao, H. Nakai, T. Vreven, J. A. Montgomery, Jr., J. E. Peralta, F. Ogliaro, M. Bearpark, J. J. Heyd, E. Brothers, K. N. Kudin, V. N. Staroverov, T. Keith, R. Kobayashi, J. Normand, K. Raghavachari, A. Rendell, J. C. Burant, S. S. Iyengar, J. Tomasi, M. Cossi, N. Rega, J. M. Millam, M. Klene, J. E. Knox, J. B. Cross,V. Bakken, C. Adamo, J. Jaramillo, R. Gomperts, R. E. Stratmann, O. Yazyev, A. J. Austin, R. Cammi, C. Pomelli, J. W. Ochterski, R. L. Martin, K. Morokuma, V. G. Zakrzewski, G. A. Voth, P. Salvador, J. J. Dannenberg, S. Dapprich, A. D. Daniels, O. Farkas, J. B. Foresman, J. V. Ortiz, J. Cioslowski, and D. J. Fox, Gaussian 09, Revision D.01, Gaussian, Inc., Wallingford CT, 2013.

Graphical Abstract

Pyrene thiazole-conjugate as ratiometric chemosensor with high selectivity and sensitivity for tin (Sn^{4+}) and its application in imaging live cells

Ajit Kumar Mahapatra*, Sanchita Mondal, Kalipada Maiti, Saikat Kumar Manna, Rajkishor Maji, Debasish Mondal, Sukhendu Mandal, Shyamaprosad Goswami, Ching Kheng Quah and Hoong-Kun Fun

A new pyrene thiazole-conjugate amine based fluoroionophore, **PTC** was developed for ratiometric detection of Sn^{4+} ion in organo-aqueous medium.